

Monte Carlo Quench Action approach for integrable spin chains

Vincenzo Alba¹, Pasquale Calabrese¹

¹ International School for Advanced Studies (SISSA), Via Bonomea 265, 34136, Trieste, Italy, INFN, Sezione di Trieste

Abstract.

fdasfa

1. Introduction

We show that it is possible to numerically simulate the Quench Action approach combining Monte Carlo methods and Bethe ansatz techniques.

We focus on the situation in which the pre-quench initial state is the Neel state or the Majumdar-Ghosh state.

We investigate the importance of the zero-momentum strings in the Quench Action.

Without zero-momentum strings the overlap saturation rules are not valid, i.e., in finite size systems the vast majority of the eigenstates contain zero momentum strings.

The details on the eigenstates counting depend on the pre-quench initial state.

However, we show that one can restrict to the set of non-zero momentum strings. The fact that one neglects zero-momentum strings gives rise only to scaling corrections.

We also investigate the validity of the Bethe-Takahashi approximation for the calculation of the overlap.

2. The Heisenberg spin chain

Here we consider the spin- $\frac{1}{2}$ isotropic Heisenberg chain (XXX chain). The XXX chain with L sites is defined by the Hamiltonian

$$\mathcal{H} \equiv J \sum_{i=1}^L \left[\frac{1}{2} (S_i^+ S_{i+1}^- + S_i^- S_{i+1}^+) + S_i^z S_{i+1}^z \right], \quad (1)$$

where $S_i^\pm \equiv (\sigma_i^x \pm i\sigma_i^y)/2$ are spin operators acting on the site i , $S_i^z \equiv \sigma_i^z/2$, and $\sigma_i^{x,y,z}$ the Pauli matrices. We fix $J = 1$ and use periodic boundary conditions, identifying sites $L+1$ and 1 . The total magnetization $S_T^z \equiv \sum_i S_i^z = L/2 - M$, with M number of down spins (particles), commutes with (1), and it is here used to label its eigenstates.

2.1. Bethe equations and wavefunctions

The generic eigenstate of (1) in the sector with M particles can be written as

$$|\Psi_M\rangle = \sum_{1 \leq x_1 < x_2 < \dots < x_M \leq L} A_M(x_1, x_2, \dots, x_M) |x_1, x_2, \dots, x_M\rangle, \quad (2)$$

where the sum is over the positions $\{x_i\}$ of the particles, and $A_M(x_1, x_2, \dots, x_M)$ is the eigenstate amplitude corresponding to particles at positions x_1, x_2, \dots, x_M . $A_M(x_1, x_2, \dots, x_M)$ is given as

$$A_M(x_1, x_2, \dots, x_M) \equiv \sum_{\mathcal{P} \in S_M} \exp \left[i \sum_{j=1}^M k_{\mathcal{P}_j} x_j + i \sum_{i < j} \theta_{\mathcal{P}_i \mathcal{P}_j} \right]. \quad (3)$$

Here the outermost sum is over the permutations S_M of the so-called quasi-momenta $\{k_1, k_2, \dots, k_M\}$. The two-particle scattering phases $\theta_{m,n}$ are defined as

$$\theta_{m,n} \equiv \frac{1}{2i} \log \left[- \frac{e^{ik_m + ik_n} - 2e^{ik_m} + 1}{e^{ik_m + ik_n} - 2e^{ik_n} + 1} \right]. \quad (4)$$

The energy associated to the eigenstate (2) is

$$E = \sum_{\alpha=1}^M (\cos(k_\alpha) - 1). \quad (5)$$

The quasi-momenta $\{k_\alpha\}$ are obtained by solving the so-called Bethe equations

$$e^{ik_\alpha L} = \prod_{\beta \neq \alpha}^M \left[-\frac{1 - 2e^{ik_\alpha} - e^{ik_\alpha + ik_\beta}}{1 - 2e^{ik_\beta} - e^{ik_\alpha + ik_\beta}} \right]. \quad (6)$$

It is useful to introduce the rapidities $\{\lambda_\alpha\}$ as

$$k_\alpha = \pi - 2 \arctan(\lambda_\alpha) \pmod{2\pi}. \quad (7)$$

Taking the logarithm on both sides in (6), and using (7), one obtains the Bethe equations in logarithmic form as

$$\arctan(\lambda_\alpha) = \frac{\pi}{L} J_\alpha + \frac{1}{L} \sum_{\beta \neq \alpha} \arctan\left(\frac{\lambda_\alpha - \lambda_\beta}{2}\right), \quad (8)$$

where $-L/2 < J_\alpha \leq L/2$ are the so-called Bethe quantum numbers. The J_α are half-integers and integers for $L - M$ even and odd.

These solutions of the Bethe equations (6) form particular “string” patterns in the complex plane, in the limit of large chains $L \rightarrow \infty$ (string hypothesis) [?, ?]. Specifically, rapidities forming a “string” of length $1 \leq n \leq M$ (that we defined here as n -string) are parametrized as

$$\lambda_{n;\gamma}^j = \lambda_{n;\gamma} - i(n - 1 - 2j) + i\delta_{n;\gamma}^j, \quad j = 0, 1, \dots, n - 1, \quad (9)$$

where $\lambda_{n;\gamma}$ is the real part of the string (string center), and γ labels strings with different centers, while j labels the different components of the string. In (9) $\delta_{n;\gamma}^j$ are the string deviations, which typically vanish exponentially in the thermodynamic limit.

Notice that pure real rapidities are strings of unit length (1-strings).

2.2. Bethe-Takahashi equations.

The string centers $\lambda_{n;\gamma}$ in (9) are obtained by solving the so-called Bethe-Takahashi equations

$$2L\theta_n(\lambda_{n;\gamma}) = 2\pi I_{n;\gamma} + \sum_{(m,\beta) \neq (n,\gamma)} \Theta_{m,n}(\lambda_{n;\gamma} - \lambda_{m;\beta}), \quad (10)$$

where the generalized scattering phases $\Theta_{m,n}$ read

$$\Theta_{m,n}(x) \equiv \begin{cases} \theta_{|n-m|}(x) + \sum_{r=1}^{(n+m-|n-m|-1)/2} 2\theta_{|n-m|+2r}(x) + \theta_{n+m}(x) & \text{if } n \neq m \\ \sum_{r=1}^{n-1} 2\theta_{2r}(x) + \theta_{2n}(x) & \text{if } n = m \end{cases}$$

and $\theta_\alpha(x) \equiv 2 \arctan(x/\alpha)$. Here $I_{n;\gamma}$ are the Bethe-Takahashi quantum numbers associated with $\lambda_{n;\gamma}$.

Each M -particle eigenstate can be characterized by its “string content” $\mathcal{S} \equiv \{s_1, \dots, s_M\}$, with s_n the number of n -strings.

It can be shown that $I_{n;\gamma}$ are integers or half-integers for $L - s_n$ odd and even, respectively.

Clearly, the constraint $\sum_{\alpha=1}^M \alpha s_\alpha = M$ has to be satisfied. The upper bound for the Bethe-Takahashi quantum numbers can be derived as

$$|I_{n;\gamma}| \leq I_n^{(MAX)} \equiv \frac{1}{2}(L - 1 - \sum_{m=1}^M t_{m,n} s_m), \quad (11)$$

where $t_{m,n} \equiv 2\min(n, m) - \delta_{m,n}$.

3. Overlap with the Neel state

Here we restrict to the parity-invariant eigenstates. These are the only eigenstates with non-zero overlap with the Neel state. Parity-invariant eigenstates contain only pairs of rapidities with opposite sign.

We denote the generic parity invariant eigenstate as $|\{\pm\lambda_j\}_{j=1}^m, n_\infty\rangle$, where m is the number of rapidity pairs, N_∞ is the number of infinite rapidities, with $M = L/2 = N_\infty + 2m$, and $n_\infty \equiv N_\infty/L$ is the density of infinite rapidities.

The overlap with the Neel state $|N\rangle$ reads

$$\frac{\langle N | \{\pm\lambda_j\}_{j=1}^m, n_\infty \rangle}{||\{\lambda_j\}_{j=1}^m, n_\infty\rangle||} = \frac{\sqrt{2}N_\infty!}{\sqrt{(2N_\infty)!}} \left[\prod_{j=1}^m \frac{\sqrt{\lambda_j^2 + 1}}{4\lambda_j} \right] \sqrt{\frac{\det_m(G^+)}{\det_m(G^-)}} \quad (12)$$

where

$$G_{jk}^\pm = \delta_{jk} \left(N K_{1/2}(\lambda_j) - \sum_{l=1}^m K_1^+(\lambda_j, \lambda_l) \right) + K_1^\pm(\lambda_j, \lambda_k), \quad j, k = 1, \dots, m \quad (13)$$

and

$$K_1^\pm(\lambda, \mu) = K_1(\lambda - \mu) \pm K_1(\lambda + \mu) \quad (14)$$

and

$$K_\alpha(\lambda) \equiv \frac{8\alpha}{\lambda^2 + 4\alpha^2} \quad (15)$$

3.1. Reduced Neel overlap

Here we consider the overlap formula for the Neel state (12) in the limit $L \rightarrow \infty$, assuming that the rapidities form perfect strings.

In the case of perfect strings the matrices G_{jk}^\pm become ill-defined. Precisely, $K_1^\pm(\lambda, \mu)$ diverges if λ and μ are successive members of the same string, i.e., $|\lambda - \mu| = 2i$.

It is possible to rewrite (12) in terms of the string centers $\lambda_{n;\alpha}$ only. Here we restrict ourselves to rapidity configurations with no zero-momentum strings. Our results are not valid for zero-rapidity strings. These would require the knowledge of the precise form of

the string deviations, i.e., the dependence of the string deviations on L , as it has been pointed out in Ref. [1].

It is convenient to split the indices i, j of G_{ij}^\pm as $i = (n, \alpha)$ $j = (m, \beta)$, with n, m being the length of the strings and α, β labelling the string centers.

The result reads

$$\frac{1}{2}G_{(n,\alpha)(m,\beta)}^+ = \begin{cases} L\theta'_n(\lambda_{n;\alpha}) - \sum_{(\ell,\gamma) \neq (n,\alpha)} (\Theta'_{n,\ell}(\lambda_{n;\alpha} - \lambda_{\ell;\gamma}) + \Theta'_{n,\ell}(\lambda_{n;\alpha} + \lambda_{\ell;\gamma})) & \text{if } (n, \alpha) = (m, \beta) \\ \Theta'_{n,m}(\lambda_{n;\alpha} - \lambda_{m;\beta}) + \Theta'_{n,m}(\lambda_{n;\alpha} + \lambda_{m;\beta}) & \text{if } (n, \alpha) \neq (m, \beta) \end{cases} \quad (16)$$

Here $\theta'_n(x) \equiv d/dx \theta_n(x) = 2n/(n^2 + x^2)$ and $\Theta'(x) \equiv d/dx \Theta(x)$.

For G_{ij}^- one obtains

$$\frac{1}{2}G_{(n,\alpha)(m,\beta)}^- = \begin{cases} (L-1)\theta'_n(\lambda_{n;\alpha}) - 2 \sum_{k=1}^{n-1} \theta'_k(\lambda_{n;\alpha}) - \sum_{(\ell,\gamma) \neq (n,\alpha)} (\Theta'_{n,\ell}(\lambda_{n;\alpha} - \lambda_{\ell;\gamma}) + \Theta'_{n,\ell}(\lambda_{n;\alpha} + \lambda_{\ell;\gamma})) & \text{if } (n, \alpha) = (m, \beta) \\ \Theta'_{n,m}(\lambda_{n;\alpha} - \lambda_{m;\beta}) - \Theta'_{n,m}(\lambda_{n;\alpha} + \lambda_{m;\beta}) & \text{if } (n, \alpha) \neq (m, \beta) \end{cases}$$

Finally, the multiplicative prefactor in (12) for the generic n -string can be rewritten as

$$\prod_{a=1}^n \frac{\sqrt{(\lambda_{n;\alpha}^a)^2 + 1}}{4\lambda_{n;\alpha}^a} = \frac{1}{4^n} \left(\frac{\sqrt{n^2 + \lambda_{n;\alpha}^2}}{\lambda_{n;\alpha}} \prod_{k=0}^{[n/2]-1} \frac{(2k)^2 + \lambda_{n;\alpha}^2}{(2k+1)^2 + \lambda_{n;\alpha}^2} \right)^{\mathcal{P}}, \quad (18)$$

with $\mathcal{P} = +$ and $\mathcal{P} = -$ for even and odd strings, respectively.

4. Overlap with the Majumdar-Ghosh state

The overlap between the generic eigenstate of the XXX chain and the Majumdar-Ghosh state is obtained from the overlap with the Neel state as

$$\langle MG | \{\lambda_j\}_{j=1}^M \rangle = \prod_{j=1}^M \frac{1}{\sqrt{2}} \left(1 - \frac{\lambda_j - i}{\lambda_j + i} \right) \langle N | \{\lambda_j\}_{j=1}^M \rangle \quad (19)$$

The multiplicative factor in (19), using the string hypothesis for the generic n -string is rewritten as

$$\prod_{j=1}^M \frac{1}{\sqrt{2}} \left(1 - \frac{\lambda_j - i}{\lambda_j + i} \right) = 2^n \prod_{k=0}^{[n/2]} \frac{1}{[\lambda_{n;\gamma}^2 + (2k + (1 - (-1)^n)/2)^2]^2} \quad (20)$$

4.1. Counting of eigenstates with non-zero Neel overlap

We numerically checked that the number of states with non-zero overlap with the Neel state is given as

$$Z_{Neel} = 2^{\frac{L}{2}-1} + \frac{1}{2} B\left(\frac{L}{2}, \frac{L}{4}\right) + 1, \quad (21)$$

with $B(x, y)$ denoting the binomial coefficient. The contribution 1 accounts for the ferromagnetic state. Here we assumed that L is divisible by four. Here Z_N is obtained as the total number of parity-invariant Bethe-Gaudin-Takahashi quantum numbers.

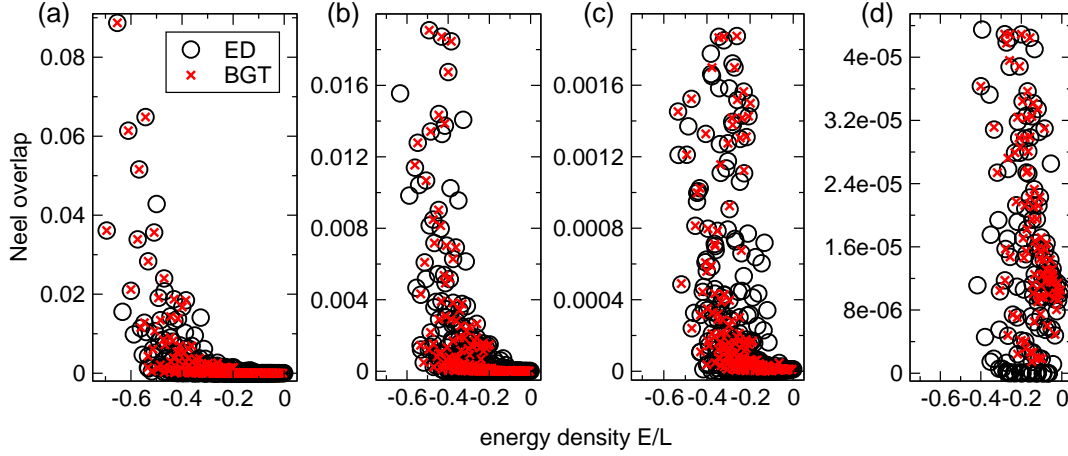


Figure 1. The squared overlap $|\langle \Psi_0 | \{\lambda \} \rangle|^2$ between the the Neel state $|\Psi_0\rangle$ and the eigenstates $|\{\lambda\}\rangle$ of the XXX chain with $L = 22$ sites. Only non-zero overlaps are shown. In all the panels the x -axis shows the eigenstate energy density E/L . The circles are the exact diagonalization results for all the non-zero overlaps. The crosses are the Bethe ansatz results obtained using the Bethe-Gaudin-Takahashi equations. The missing crosses correspond to eigenstates containing zero-momentum strings. (a) Overview of all the non-zero overlaps. (b)(c)(d) The same overlaps as in (a) zooming in the regions $[0, 0.2]$, $[0, 0.020]$, and $[0, 4 \cdot 10^{-5}]$. The discrepancies between the ED and the Bethe ansatz results are attributed to the string deviations.

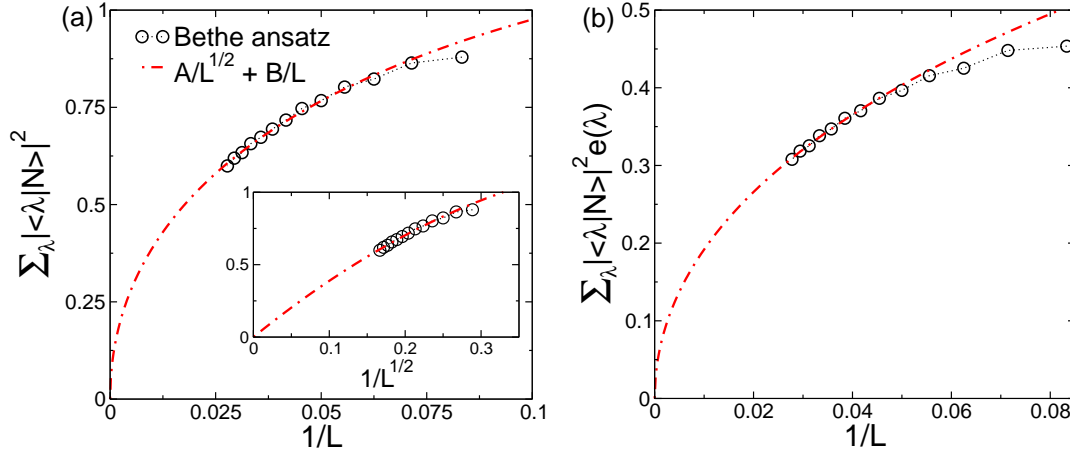


Figure 2. Overlap sum rules for the Neel state. (a) The overlap sum rule $\sum_{\{\lambda\}} |\langle \{\lambda\} | N \rangle|^2 = 1$, with $|N\rangle$ the Neel state and $|\{\lambda\}\rangle$ the eigenstates of the XXX spin chain. The x -axis shows $1/L$, with L the chain length. The circles are Bethe ansatz results for chains up to $L = 36$. The results are obtained via a full scanning of the chain Hilbert space. Only the eigenstates with no zero-momentum strings are considered. The dash-dotted line is a fit to $A/L^{1/2} + B/L$, with A, B fitting parameters. Inset: The same data as in the main Figure plotted versus $1/L^{1/2}$. (b) The same as in (a) for the sum rule $\sum_{\{\lambda\}} |\langle \{\lambda\} | N \rangle|^2 e(\{\lambda\}) = 1/2$, with $e(\{\lambda\})$ the eigenstates energy density.

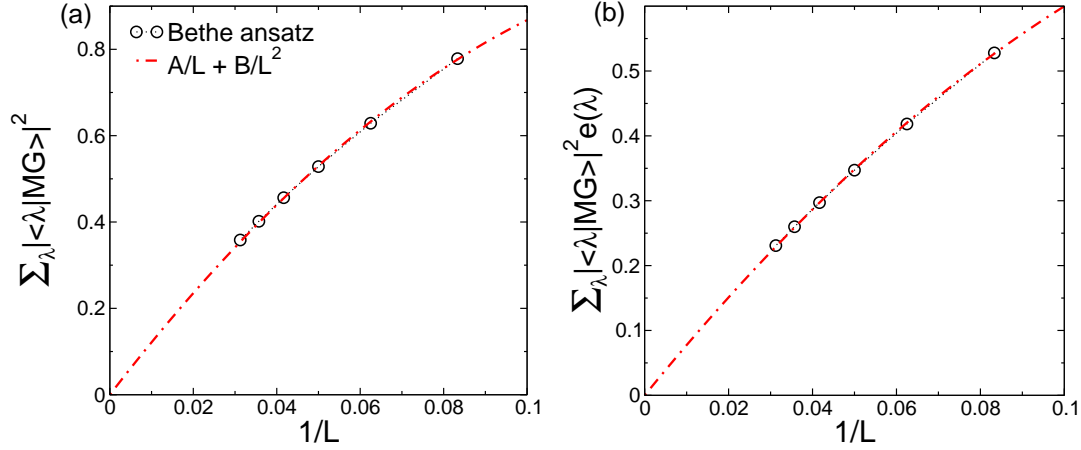


Figure 3. Overlap sum rules for the Majumdar-Ghosh (MG) state. (a) The overlap sum rule $\sum_{\{\lambda\}} |\langle \{\lambda\} | MG \rangle|^2 = 1$, with $|MG\rangle$ the Majumdar-Ghosh state and $|\{\lambda\}\rangle$ the eigenstates of the XXX spin chain. The x -axis shows $1/L$, with L the chain length. The circles are Bethe ansatz results for chains up to $L = 36$. The results are obtained via a full scanning of the chain Hilbert space. Only the eigenstates with no zero-momentum strings are considered. The dash-dotted line is a fit to $A/L + B/L^2$, with A, B fitting parameters. (b) The same as in (a) for the sum rule $\sum_{\{\lambda\}} |\langle \{\lambda\} | MG \rangle|^2 e(\{\lambda\}) = 2/3$, with $e(\{\lambda\})$ the eigenstates energy density.

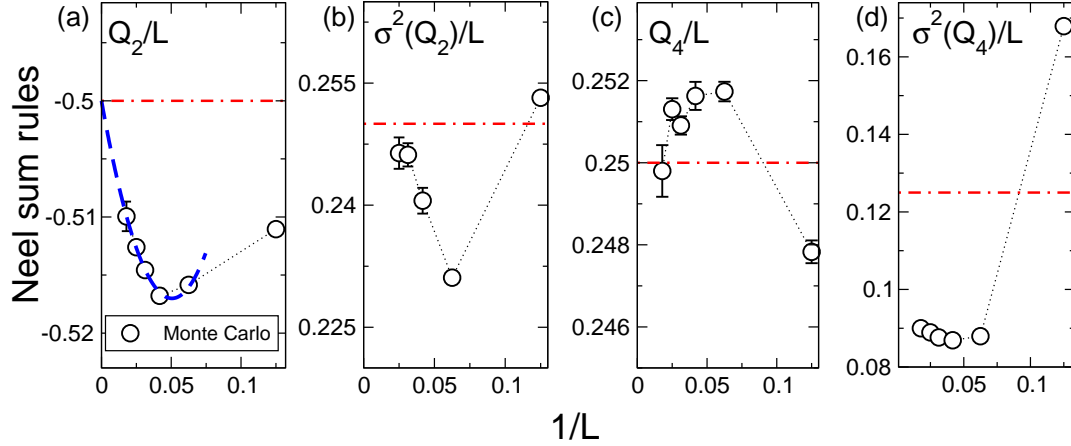


Figure 4. The overlap sum rules for the Neel state: Numerical results obtained using the Hilbert space Monte Carlo sampling approach. (a) The energy sum rule $\langle N | Q_2 | N \rangle / L = -1/2$, with Q_2/L the Hamiltonian density. We plot $\sum_{\{\lambda\}} |\langle \{\lambda\} | N \rangle|^2 Q_2(\{\lambda\}) / L = 1/2$, with $|\{\lambda\}\rangle$ the eigenstates of the XXX chain, versus the inverse chain length $1/L$. The symbols are Monte Carlo data obtained by sampling the eigenstates of the XXX chain. The dash-dotted line is the expected result. The dashed line is a fit to the behavior $-1/2 + A/L + B/L^2$, with A, B fitting parameters. (b) The energy fluctuations sum rule $\sigma^2(Q_2)/L \equiv (\langle N | Q_2^2 | N \rangle - \langle N | Q_2 | N \rangle^2) / L = 1/4$. The horizontal line is the expected result. (c)(d) Same as in (a)(b) for the charge Q_4 and its fluctuations.

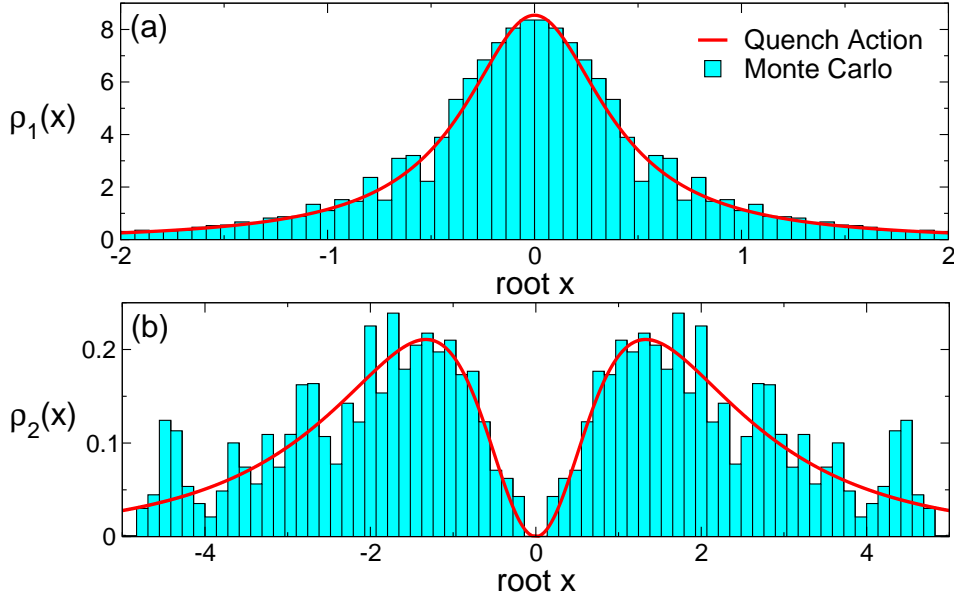


Figure 5. The steady-state root densities $\rho_1(x)$ (panel (a)) and $\rho_2(x)$ (panel (b)), plotted versus the root x . The histograms are Monte Carlo data for the Heisenberg chain with $L = 56$ sites and $\sim 10^7$ Monte Carlo steps. The y -axis is divided by 10^6 for convenience. The continuous lines are the analytical Quench-Action results in the thermodynamic limit.

After excluding the zero-momentum strings the total number of states with non-zero overlap with the Neel state is

$$\tilde{g}Z_{Neel} = \left(\frac{L}{2}, \frac{L}{4}\right) \quad (22)$$

Importantly, the fraction of eigenstates corresponding to non-zero momentum strings is vanishing in the thermodynamic limit as

$$\frac{\tilde{Z}_{Neel}}{Z_{Neel}} \propto \frac{4}{\sqrt{\pi L}}. \quad (23)$$

4.2. Eigenstates with nonzero Néel overlap: eigenstates counting and string content

Here we prove that the total number of eigenstates with Néel nonzero overlap $Z_{Neel}(L)$ for a chain of length L is given as

$$Z_{Neel} = 2^{\frac{L}{2}-1} + \frac{1}{2}B\left(\frac{L}{2}, \frac{L}{4}\right) + 1. \quad (24)$$

For simplicity here we restrict ourselves to the situation with L divisible by four. The strategy to prove (24) is to count all the possible parity-invariant BGT quantum numbers configurations. Let us consider the sector with fixed number of particles M , and a generic string content $\mathcal{S} = \{s_1, s_2, \dots, s_M\}$. Here s_n is the number of n -strings, and one has the constraint $\sum_k k s_k = M$.

It is straightforward to check that total number of parity-invariant quantum number pairs $\mathcal{N}_n(L, \mathcal{S})$ in the n -string sector is given as

$$\mathcal{N}_n(L, \mathcal{S}) = \left\lfloor \frac{L}{2} - \frac{1}{2} \sum_{m=1}^M t_{nm} s_m \right\rfloor. \quad (25)$$

where $t_{nm} \equiv 2\text{Min}(n, m) - \delta_{n,m}$. The number of parity-invariant quantum number configurations (i.e., eigenstates) $\mathcal{N}(L, \mathcal{S})$ compatible with string content \mathcal{S} is obtained by choosing in all the possible ways the parity-invariant quantum number pairs independently in each n -string sector, which implies that

$$\mathcal{N}(L, \mathcal{S}) = \prod_{m=1}^M B\left(\mathcal{N}_m, \left\lfloor \frac{s_m}{2} \right\rfloor\right). \quad (26)$$

Here the product is because each string sector is treated independently, while the factor $1/2$ in $s_m/2$ is because since all quantum numbers are organized in pairs, only half of the quantum numbers have to be specified. Note that in each n -string sector only one zero momentum (i.e., zero quantum number) string is allowed, due to the Pauli principle. Moreover, s_m is odd (even) only if the zero momentum string is (not) present. The floor function $\lfloor \cdot \rfloor$ in (26) reflects that the quantum number of zero-momentum strings is fixed.

We now consider the string configurations with particle number $0 \leq \ell \leq M$ and fixed number of strings $1 \leq q \leq M/2$. Note that the maximul allowed string length is $M/2$ beacause of parity invariance. Note also that in determining q strings of different length are treated equally. Clearly, one has that $\sum_m s_m = q$. For a given fixed pair ℓ, q the total number of quantum number configurations is given as

$$\mathcal{N}'(L, \ell, q) = \sum_{\{\{s_m\} : \sum m s_m = \ell, \sum s_m = q\}} \mathcal{N}(L, \mathcal{S}), \quad (27)$$

where the sum is over the content $\{s_m\}_{m=1}^M$ compatible with the constraints $\sum_m s_m = q$ and $\sum_m m s_m = \ell$. The strategy is to write a recursive relation for $\mathcal{N}'(L, \ell, q)$. To this purpose it is useful to consider the shifted string content \mathcal{S}' defined as

$$\mathcal{S}' \equiv \{s_{m+1}\} \quad \text{with } s_m \in \mathcal{S}, \forall m. \quad (28)$$

Using the definition of t_{ij} , it is straightforward to derive that

$$t_{ij} = t_{i-1, j-1} + 2, \quad (29)$$

which implies that $\mathcal{N}_n(L, \mathcal{S})$ (see (25)) satisfies the recursive equation

$$\mathcal{N}_n(L, \mathcal{S}) = \mathcal{N}_{n-1}(L - 2q, \mathcal{S}'). \quad (30)$$

After substituting in (26) one obtains

$$\mathcal{N}(L, \mathcal{S}) = B\left(\mathcal{N}_1(L, \mathcal{S}), \left\lfloor \frac{s_1}{2} \right\rfloor\right) \mathcal{N}(L - 2q, \mathcal{S}'). \quad (31)$$

Finally, after substituting (31) in (27), one obtains a recursive relation for $\mathcal{N}'(L, \ell, q)$ as

$$\mathcal{N}'(L, \ell, q) = \sum_{s=0}^{q-1} B\left(\frac{L}{2} - q + \left\lfloor \frac{s}{2} \right\rfloor, \left\lfloor \frac{s}{2} \right\rfloor\right) \mathcal{N}'(L - 2q, \ell - q, q - s), \quad (32)$$

with the constraint that when $\ell = q$ one has

$$\mathcal{N}'(L, q, q) = B\left(\left\lfloor \frac{L-q}{2} \right\rfloor, \left\lfloor \frac{q}{2} \right\rfloor\right). \quad (33)$$

This is obtained by observing that if $\ell = q$ only 1-strings are allowed and (25) gives $\mathcal{N}_n(L, \mathcal{S}) = \lfloor (L-q)/2 \rfloor$.

It is straightforward to check that for even q the ansatz

$$\mathcal{N}'(L, \ell, q) = \frac{q}{\ell} B\left(\frac{L-\ell}{2}, \frac{q}{2}\right) B\left(\frac{\ell}{2}, \frac{q}{2}\right), \quad (34)$$

satisfies (32). For odd q the solution of (32) is

$$\mathcal{N}'(L, \ell, q) = \frac{\ell - q + 1}{\ell} B\left(\frac{L-\ell}{2}, \frac{q-1}{2}\right) B\left(\frac{\ell}{2}, \frac{q-1}{2}\right). \quad (35)$$

The number of eigenstates in the sector with ℓ particles with nonzero Néel overlap $Z'_{Neel}(L, \ell)$ are obtained by summing over all possible values of q as

$$Z'_{Neel}(L, \ell) = \sum_{q=1}^{\ell} \mathcal{N}'(L, \ell, q). \quad (36)$$

It is convenient to split the summation in (36) considering odd values of q and even q separately. For odd q one obtains

$$\sum_{k=0}^{\ell/2-1} \mathcal{N}'(L, \ell, 2k+1) = B\left(\frac{L}{2} - 1, \frac{\ell}{2} - 1\right), \quad (37)$$

while for even q one has

$$\sum_{k=0}^{\ell/2} \mathcal{N}'(L, \ell, 2k) = B\left(\frac{L}{2} - 1, \frac{\ell}{2}\right). \quad (38)$$

Putting everything together one obtains

$$Z'_{Neel}(L, \ell) = B\left(\frac{L}{2} - 1, \frac{\ell}{2} - 1\right) + B\left(\frac{L}{2} - 1, \frac{\ell}{2}\right). \quad (39)$$

The total number of eigenstates with nonzero Néel overlap $Z_{Neel}(L)$ (cf. (24)) is obtained from (39) by summing over the allowed values of $\ell = 2k$ with $k = 0, 1, \dots, \ell/2$.

4.3. Excluding the zero-momentum strings

Here we demonstrate that the total number of eigenstates with nonzero Néel overlap, which do not contain zero-momentum strings, $\tilde{Z}_{Neel}(L)$ is given as

$$\tilde{Z}_{Neel}(L) = B\left(\frac{L}{2}, \frac{L}{4}\right). \quad (40)$$

Given a generic M -particle eigenstate of the XXX chain, due to parity invariance, if one excludes the zero-momentum strings only n -strings with length $n \leq M/2$ are allowed. Similarly, the string content is of the form $\tilde{\mathcal{S}} \equiv \{\tilde{s}_1, \dots, \tilde{s}_{M/2}\}$, i.e., $\tilde{s}_m = 0 \ \forall m > M/2$. Note that due to parity invariance and to the exclusion of the zero-momentum strings one has that \tilde{s}_m is always an even integer. Clearly one has $\sum_{m=1}^{M/2} m \tilde{s}_m = M$.

The total number of parity-invariant quantum numbers $\tilde{\mathcal{N}}_n$ in the n -string sector is given as

$$\tilde{\mathcal{N}}_n(L, \tilde{\mathcal{S}}) = \frac{L}{2} - \frac{1}{2} \sum_{m=1}^{M/2} t_{nm} \tilde{s}_m. \quad (41)$$

The proof now proceeds as in 4.2. One can define the total number of eigenstates with nonzero Néel overlap in the sector with ℓ particles and q different strings as $\tilde{\mathcal{N}}'(L, \ell, q)$. Note that due to parity invariance and the exclusion of zero-momentum strings, q must be even. It is straightforward to show that $\tilde{\mathcal{N}}'(L, \ell, q)$ obeys the recursive relation

$$\tilde{\mathcal{N}}'(L, \ell, q) = \sum_{s=0}^{q/2-1} B\left(\frac{L}{2} - q + s, s\right) \tilde{\mathcal{N}}'\left(L - 2q, \frac{\ell - q}{2}, \frac{q}{2} - s\right), \quad (42)$$

with the constraint

$$\tilde{\mathcal{N}}'(L, 1, 1) = \frac{L}{2} - 1. \quad (43)$$

It is straightforward to check that the solution of (42) is given as

$$\tilde{\mathcal{N}}'(L, \ell, q) = \frac{L - 2\ell + 2}{L - \ell + 2} B\left(\frac{L - \ell}{2} + 1, q\right) B\left(\frac{\ell}{2} - 1, \frac{q}{2} - 1\right). \quad (44)$$

After summing over the allowed values of $q = 2k$ with $k = 1, 2, \dots, \ell/2$ one obtains the total number of eigenstates with nonzero Néel overlap at fixed number of particles ℓ $\tilde{Z}'_{Neel}(L, \ell)$ as

$$\tilde{Z}'_{Neel}(L, \ell) = B\left(\frac{L}{2}, \frac{\ell}{2}\right) - B\left(\frac{L}{2}, \frac{\ell}{2} - 1\right). \quad (45)$$

Summing over ℓ one obtains (22).

[1] P. Calabrese and P. Le Doussal, J. Stat. Mech. (2014) P05004.

Bethe states with nonzero Néel overlap ($N = 12$)				
String content	$2I_n^+$	E	$ \langle\{\lambda\} \Psi_0\rangle ^2$	here
6 inf	-	0	0.002164502165	0.002164502165
2 one, 4 inf	1_1	-3.918985947229	0.096183409244	0.096183409244237
	3_1	-3.309721467891	0.011288497947	0.0112884979464673
	5_1	-2.284629676547	0.004542580506	0.0045425805061850
	7_1	-1.169169973996	0.002752622983	0.0027526229835876
	9_1	-0.317492934338	0.002116006203	0.0021160062026402
4 one, 2 inf	$1_1 3_1$	-7.070529325964	0.310133033838	0.554809782804
	$1_1 5_1$	-5.847128730477	0.129277023687	
	$1_1 7_1$	-4.570746557876	0.085992436024	
	$3_1 5_1$	-5.153853093221	0.015256395523	
	$3_1 7_1$	-3.916336243695	0.010091113504	
	$5_1 7_1$	-2.817696043731	0.004059780228	
2 two, 2 inf	1_2	-1.905667167442	0.001207238321	0.005468702625
	3_2	-1.368837200825	0.002340453815	
	5_2	-0.681173793635	0.001921010489	
1 one, 1 three, 2 inf	$0_1 0_3$	-2.668031843135	0.034959609810	0.034959609810
6 one	$1_1 3_1 5_1$	-8.387390917445	0.153412152966	0.153412152966
2 two, 2 one	$1_1 1_2$	-5.401838225870	0.040162686361	0.046134750850
	$3_1 1_2$	-4.613929948329	0.004636541934	
	$5_1 1_2$	-3.147465758841	0.001335522556	
1 three, 3 one	$0_1 2_1 0_3$	-6.340207488736	0.052743525774	0.078910020729
	$0_1 4_1 0_3$	-5.203653009936	0.015022005621	
	$0_1 6_1 0_3$	-3.788693957250	0.011144489334	
1 five, 1 one	$0_1 0_5$	-2.444293750583	0.005887902992	0.005887902992
2 three	1_3	-1.111855930538	0.001342476001	0.001342476001
1 two, 1 four	$0_2 0_4$	-1.560671012472	0.000026982174	0.000026982174

Table 1. All Bethe states for $N = 12$ with nonzero overlap with the zero-momentum Néel state. The overlap squares add up to 1 up to the precision in which the Bethe equations were solved. The $2I_n^+$ in the second column give the positive n -string quantum numbers of the parity-invariant Bethe states.

Bethe states with nonzero M-G overlap ($L = 12$)			
String content	Energy (ED)	$ \langle\{\lambda\} \Psi_0\rangle ^2$ (ED)	$ \langle\{\lambda\} \Psi_0\rangle ^2$ (B-T)
$1_1 3_1 5_1$	-8.38739	0.716616	0.7166157692239
	-6.34021	0.205891	
$5_1 1_2$	-5.40184	0.0556247	0.05403336654338
	-5.20365	0.0388322	
$3_1 1_2$	-4.61393	0.00568743	0.005582983043235
	-3.78869	0.00601941	
$1_1 1_2$	-3.14747	0.00210748	0.0021070869333835
	-2.44429	0.000129601	
	-1.56067	0.000330573	
1_3	-1.11186	0.0000117278	0.000012785579923275

Table 2. All Bethe states for $L = 12$ with nonzero overlap with the zero-momentum M-G state. The first column show the string content of the eigenstate. The second and third columns show the exact diagonalization results for the energy and the overlap, respectively. The last column is the overlap obtained in the Bethe ansatz approach using the Bethe-Takahashi equations.

Bethe states with nonzero M-G overlap ($L = 16$)			
String content	Energy (ED)	$ \langle\{\lambda\} \Psi_0\rangle ^2$ (ED)	$ \langle\{\lambda\} \Psi_0\rangle ^2$ (B-T)
$7_1 5_1 3_1 1_1$	-11.1423	0.517742	0.5177418283152
	-9.59129	0.244845	
$7_1 5_1 1_2$	-8.81424	0.0727096	0.07100180464371
	-8.56579	0.082852	
$7_1 3_1 1_2$	-7.96995	0.0232953	0.02300602650371
	-7.89112	0.0181713	
$7_1 1_1 1_2$	-7.51522	0.00245007	0.002427999643379
	-7.41983	0.0192443	
$5_1 3_1 1_2$	-6.80829	0.012519	0.012518660407092
	-6.78357	0.00398018	
$5_1 1_1 1_2$	-6.3398	0.00135119	0.0013511980854654
	-6.25276	0.000721952	
	-5.86683	0.00112415	
	-5.69103	0.000141052	
$3_1 1_2$	-5.50802	0.00373666	
	-5.45276	0.000466819	0.0004668223478716
	-5.06385	0.000380056	0.000166548883431
	-4.86668	0.0000395855	
	-4.64743	0.000014786	0.000016403668846624
	-4.49059	0.00155894	
	-4.25924	0.000109932	
	-3.93068	$4.12108e - 6$	$4.6283550855711e - 6$
	-3.92645	0.0000102752	
	-3.77995	0.0000732808	
	-3.259	0.0000348879	
	-3.12751	0.0000739906	0.00007017294942524
	-3.04176	$1.62543e - 6$	
	-3.00072	$1.4684e - 6$	$1.6374806913113e - 6$
	-2.32465	$2.01172e - 8$	
	-2.26529	$7.53377e - 6$	
	-2.02465	$5.8028e - 7$	$5.722094498217e - 7$
	-1.38078	$2.17607e - 7$	
	-1.11438	$1.825e - 7$	
	-0.844856	$1.84715e - 9$	$2.4957509639475e - 9$

Table 3. All Bethe states for $L = 12$ with nonzero overlap with the zero-momentum M-G state. The first column show the string content of the eigenstate. The second and third columns show the exact diagonalization results for the energy and the overlap, respectively. The last column is the overlap obtained in the Bethe ansatz approach using the Bethe-Takahashi equations.